

Assessment of ASCE 7-10 for wind effects on low-rise wood frame buildings with database-assisted design methodology

Jing He¹, Fang Pan² and C.S. Cai^{*1}

¹Department of Civil and Env. Eng., Louisiana State University, Baton Rouge, LA 70803, USA

²Southwest Research Institute, San Antonio, TX 78228, USA

(Received September 10, 2017, Revised January 30, 2018, Accepted March 6, 2018)

Abstract. The design wind pressure for low-rise buildings in the ASCE 7-10 is defined by procedures that are categorized into the Main Wind Force-Resisting System (MWFRS) and the Components and Cladding (C&C). Some of these procedures were originally developed based on steel portal frames of industrial buildings, while the residential structures are a completely different structural system, most of which are designed as low-rise light-frame wood constructions. The purpose of this study is to discuss the rationality (or irrationality) of the extension of the wind loads calculated by the ASCE 7-10 to the light-frame wood residential buildings that represent the most vulnerable structures under extreme wind conditions. To serve this purpose, the same approach as used in the development of Chapter 28 of the ASCE 7-10 that envelops peak responses is adopted in the present study. Database-assisted design (DAD) methodology is used by applying the dynamic wind loads from Louisiana State University (LSU) database on a typical residential building model to assess the applicability of the standard by comparing the induced responses. Rather than the postulated critical member demands on the industrial building such as the bending moments at the knee, the maximum values at the critical points for wood frame buildings under wind loads are used as indicators for the comparison. Then, the critical members are identified through these indicators in terms of the displacement or the uplift force at connections and roof envelope. As a result, some situations for each of the ASCE 7 procedures yielding unconservative wind loads on the typical low-rise residential building are identified.

Keywords: aerodynamics; buildings; low-rise; databases; structural designs; wind forces; wind tunnels; ASCE; standards and codes

1. Introduction

In North America, above 90% of residential buildings are designed as light-frame wood constructions (van de Lindt and Dao 2009). As reported by Pielke and Landsea (1998), the United States has at least a one-in-six chance of suffering hurricane-induced damage of at least \$10 billion (in normalized 1996 dollars) each year. The vast majority of these damages are the result of the failure of wood-frame residential houses (Sparks 1991). Specifically, in 1992, Hurricane Andrew resulted in \$26.5 billion economic loss, which marked the largest loss caused by a natural disaster that the United States had ever experienced at that time. The inadequate performance of houses during Hurricane Andrew prompted improvements in detection capability for storms and the upgrade of building codes and standards (Cook and Soltani 1994). Although the buildings constructed with the upgraded code had a “clearly superior performance” as indicated by Reinhold (2005), the code of practice is still insufficient as observed in 2005 Hurricane Katrina that resulted in \$108 billion of damage partly caused by the wind hazard, though mainly due to storm surge, and broke the most destructive and costliest storm record in the history of the United States. Substantial

improvements and strengthening are to be made on the basis for and the process of the codification of wind loads. However, for serving as a design standard that must be practical for engineers and construction workers, simplifications that would induce the overestimation and/or underestimation of the wind effects are inevitable to avoid bulky documents with overly complex provisions. Thus, this study takes another perspective to reinvestigate the adequacy of the ASCE 7-10 in the structural response prediction on light-frame wood houses, which requires an appreciation of the methodologies that lead to the current provisions.

The ASCE 7 allows for the design wind loads on different components of a low-rise building that are categorized into the Main Wind Force-Resisting System (MWFRS) and the components and cladding (C&C). The wind loads for MWFRS can be determined by using either the Envelope Procedure or the Directional Procedure on the basis of the ASCE 7, also referred to as low-rise procedure and all heights procedure, respectively. The pressure coefficients developed within the framework of the Envelope Procedure are the “pseudo” loading conditions that envelop the desired critical wind effects, i.e., the peak bending moment at the knee of the two-hinged frame and three-hinged frame, bending moment at the ridge of the two-hinged frame, the total uplift, and the total horizontal shear, based on the work at the University of Western Ontario (UWO) by Davenport *et al.* (1978).

*Corresponding author, Professor
E-mail: cscail@lsu.edu

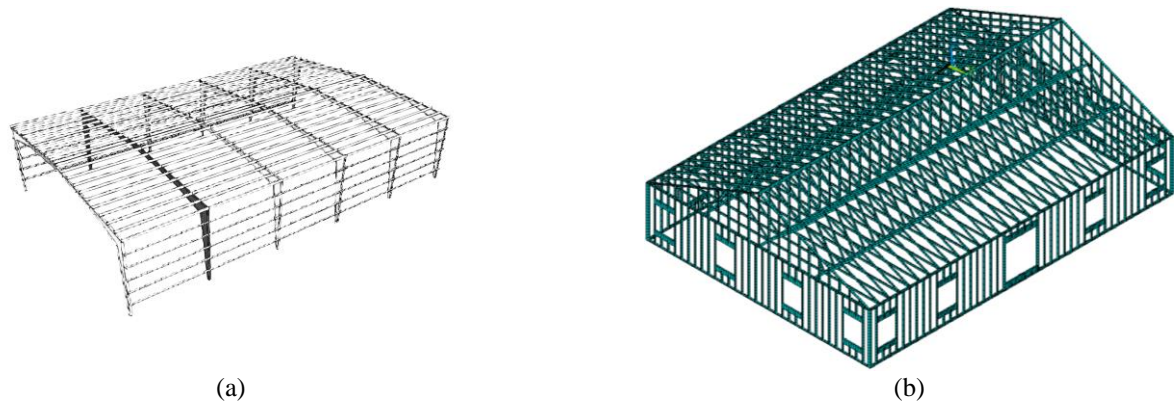


Fig. 1 Typical structural system for (a) steel frame (Coffman *et al.* 2010) and (b) light-frame low-rise wood building

As opposed to the Envelope Procedure, a more general envelope approach is adopted in the Directional Procedure, where the pressure coefficients reflect the actual peak loading on each surface of the building as a function of the wind direction. As such, it can be expected that the Envelope Procedure that is derived directly from the structural actions would predict more accurate reactions at the postulated critical members than the Directional Procedure when the configuration considered is consistent with what the provisions are developed upon. Isyumov and Case (1995) extended the application of the pseudo-pressure coefficient to another structural system, i.e., a single-story shear wall structure with a truss roof by comparing the response of it to that of a moment frames structure as used in the development of ASCE 7. Five more postulated critical structural actions are considered in accordance with the new structure type. They are the maximum shear in the north-south walls, the maximum shear in the east-west walls, the maximum uplift at truss reaction, the maximum positive member force for truss, and the maximum negative member force for the the truss. It is noted that for other structures, especially for other different types of structural systems, as suggested by Trautner and Ojdrovic (2013), there is no guarantee that the structural actions selected for the development of wind loads under the Envelope Procedure will also be critical for the design, as the structural behaviors are governed by building configurations.

The C&C consists of components (i.e., fasteners, studs, and roof trusses) and cladding (i.e., wall coverings, roof coverings, exterior windows, and door) that receive wind loads directly or from each other. The pressure coefficients for the C&C, with an attempt to address the “worst case” loading scenario on a particular member during the wind event (Douglas and Weeks 2003), are developed by using an approach that is different from the method followed by the Directional Procedure. It involves spatial and temporal averaging of point pressures over an effective area through 360° wind angles to account for the small effective area of a particular component. As such, for the pressure coefficients given in the C&C chapter, the directionality of wind has been removed, and the surfaces of the building have been “zoned” to reflect the envelope of the peak pressures in the

horizontal direction besides the vertical direction considered in the directional method of the MWFRS. The influence of exposure has also been removed since the design wind pressures for the C&C are intended to be based on the exposure category resulting in the highest wind loads for any wind direction at the site. The larger wind effects of the C&C than the MWFRS wind loads on the structural system are found by Martin *et al.* (2011) by applying both of them on a numerical model. This result is not surprising in that the spatial coherence of the pressures is greater between pressures acting over small than over large surfaces. From wind engineering perspective, the larger area that covers the MWFRS contains more vortices, each of which can be considered by its resultant force, and some of the vortices would cancel out each other, resulting in a limited resultant force. In contrast, for the C&C typically dealing with small areas, some vortices would cover the entire element, leading to the resultant forces larger than the “canceled out” values of the MWFRS.

Studies on the ASCE 7 evaluation is numerous in the literature and can be categorized into two levels by the code performance indicator: peak pressure coefficient or peak structural response that is consistent with the methodology of the Directional Procedure and the Envelope Procedure of the MWFRS, respectively. The significant underestimations based on the code procedures have repeatedly been pointed out on the pressure level, and the degree of discrepancy in the temporal and spatial averaged pressure coefficients depends on factors such as roof zone, building shape, size of the effective area, etc. (e.g., Kopp *et al.* 2005, Tieleman *et al.* 2006, Gavanski *et al.* 2013). For a safer building design, database-assisted design (DAD) is initiated to increase the accuracy of wind loads by replacing the application of the tabular pressure coefficients specified in the ASCE 7 with the direct use of pressure time histories obtained from comprehensive wind tunnel tests. Taking advantage of the development of the DAD technique, the response level approach is adopted more in recent years, and the highly non-conservative wind effects of the ASCE 7 are also recognized in the Envelope Procedure. Such risk-inconsistency is found to increase with the building height by St. Pierre *et al.* (2005) and Coffman *et al.* (2010) with the National Institute of Standards and Technology (NIST)

database, and it also increases with the increase of the roof angle as stated by Kwon *et al.* (2016) with the Tokyo Polytechnic University (TPU) database implemented by the database-enabled design module for low-rise buildings (DEDM-LR). To be consistent with the ASCE 7 Envelope Procedure, these evaluations only compare the reactions of the MWFRS and are based on industrial pre-engineered metal buildings with single-story moment resisting steel frames as shown in Fig. 1(a). The selected structural reactions in terms of influence coefficients at postulated critical members are also consistent with the critical demands in the development of the ASCE 7 as code performance indicators. However, in the case of residential structures of which over 95% are light-frame wood buildings in the U.S. (Fischer *et al.* 2009), such indicators are no more rational.

For the light wood construction (Fig. 1(b)), the predominant damage is not a structural failure, but a failure of the building envelope, such as doors, windows, and the roof systems (FEMA 2005). Once the envelope is breached, the rains accompanying a hurricane can intrude to the building resulting in major interior damage. Meanwhile, the internal pressure increases rapidly leading to a significant overloading on both the MWFRS and C&C that are probably not designed to handle. Thus, except for the strength of each structural component, the integrity of the entire building relies heavily on the adequacy of the connections between components to properly transfer the forces. The critical demands in the configuration of wood buildings under wind loads are the uplift forces along vertical load paths, particularly at roof-to-wall connection (RTWC) and the sheathing-to-truss connection (STTC) (FEMA 1993, Shanmugam *et al.* 2009, Jacklin *et al.* 2014), rather than the bending moment at the knee and ridge, etc., as considered in the development process of the ASCE 7. As such, the design of residential buildings using the ASCE 7 provisions which fail to incorporate the critical structural responses of this type of configuration would cause the wrong estimation of wind loads and result in the unexpected vulnerability of the structure during extreme wind events. To the authors' knowledge, the evaluation of the applicability of the ASCE7-10 on the wood frame residential building in terms of responses is still missing. The reason behind is partly due to the lack of having a significantly detailed and validated finite-element (FE) model. This model should be able to reflect the actual performance of wood houses under wind loads by modeling all the connections which determine the load paths and even the initial collapse, as summarized by He *et al.* (2017). According to the discussions made above, a few notes are ready for the present study:

1. The purpose of this study is to evaluate the adequacy of the ASCE 7 code-specified procedures for wind design of the residential structures that typically consist of the light-frame wood building. The wind load effect in terms of the peak pressures that are dependent on the building exterior geometry is not discussed here since they are not influenced by the load paths and therefore, cannot reflect the adequacy of the ASCE 7 to a different type of structures. Instead, a

validated numerical model with detailed component simulation such as nails is used to evaluate the ASCE 7 in the response level, i.e. the peak response.

2. Both the MWFRS (including two procedures) and the C&C methods in the ASCE 7 are applied to compare the wind effects of DAD methodology based on the pressure time histories from Louisiana State University (LSU) aerodynamic database, simply called DAD approach in some cases later on.

3. The critical demands such as the displacement /uplift force at connections and roof for the light-frame wood structure are considered as code performance indicators, rather than the bending moments for industrial buildings.

4. Some situations are identified that each of the ASCE 7 procedures yields unconservative wind loads on a typical low-rise residential building.

2. LSU aerodynamic database

2.1 Building model

A 1:50 scale building model is selected from the LSU database with the prototype being a one-story 5:12 pitched gable roof residential house with timber construction and a rectangular plan of 18.3 m by 13.4 m (60 ft by 44 ft) and overhang height of 3.0 m (9.8 ft). This configuration is designed in accordance with the South/Key CBG type that is defined in the Florida Public Hurricane Loss Model (FPHLM) and intends to be the representative of the United States residential buildings. This typical building model mainly consists of four parts: lumber frames, roof and wall sheathings, connections between sheathing and frame, frame and frame, and foundation hold-downs as they act as the critical load bearing components. Especially, unlike the past models used to evaluate the ASCE 7 standard, openings along with the induced internal pressures measured from wind tunnel tests are incorporated for the comparison of the wind effect between the ASCE 7 standard estimate and the time-history wind loading design. There are 17 openings in total, i.e., windows and doors, distributed on the walls to capture the behavior of the building subjected to internal fluctuations that lead to the over-pressurization along with the failure of the structure. More information pertaining to the opening layout and the geometric configuration can be obtained from Pan *et al.* (2013). This scaled model is mounted with 192 pressure taps (188 external taps and 3 internal taps) and connected to Scanivalve DSA3217/16Px (Serial#2100), a pressure acquisition system at a sampling rate of 500 Hz for 1 hour in full scale as shown in Fig. 2(a).

In the current study, a nonlinear numerical model is developed by using a modeling methodology for a light-frame wood structure that is validated by He *et al.* (2018). In this model, sheathing panels are represented by shell elements which are 8-noded quadrilateral with six DOF at each node to involve system effects and are built to the realistic arrangement, i.e., roof panels are staggered, and the discontinuity between the panels are taken into consideration. Frame members are modeled by 3D linear

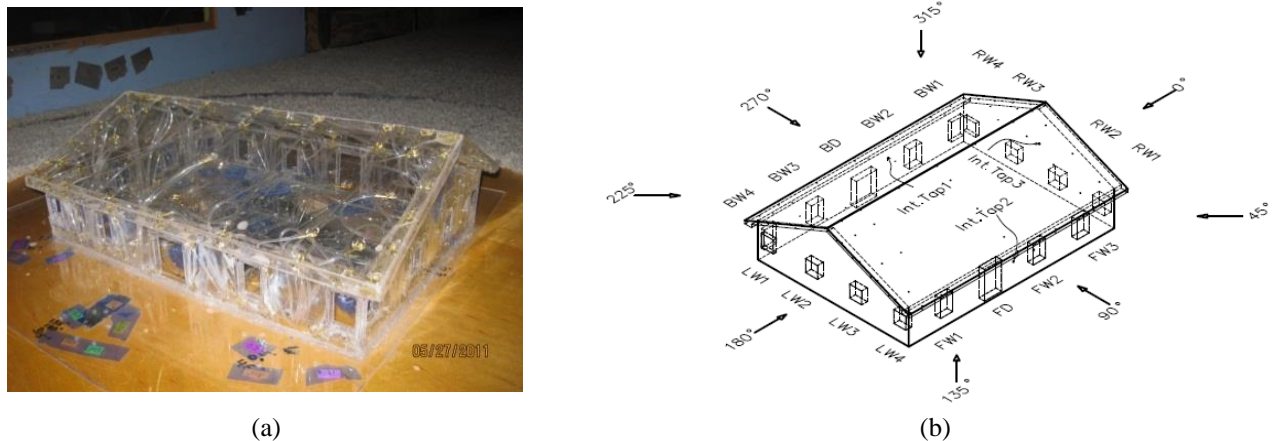


Fig. 2 Building model: (a) the experiment model tested in LSU wind tunnel and (b) the sketch of the model with the definition of wind angles investigated. (from Pan *et al.* 2013)

isotropic beam elements that are 2-noded with six DOF on each node, of which the trusses are assumed to be pinned, and the rest are considered rigid connected. The arrangement of these frame members is illustrated in Fig. 1(b). Both the sheathing and beam members are assumed to have elastic material properties. For the most critical member that usually initiates the failure of a low-rise building under wind events, the nonlinear behavior of sheathing nails is considered in this model and used as “code performance indicators” to determine how applicable of the ASCE 7 pseudo pressure coefficients to this kind of building. Each sheathing nail on the wall is modeled by three nonlinear spring elements with the force-displacement relationship in each direction to reflect the translational capacities. The rotational capacities are considered for STTCs and each of these nails is represented by six nonlinear spring elements. In this study, the roof and the sole plate are rigidly connected to the wall and the foundation, respectively. This is because the different RTWC models have negligible effect on the performance before failure (He *et al.* 2018). Since the failure stage is not discussed here, such an assumption is made to simplify the modeling. As such, continuous load paths are formed to transfer all the wind loads from the roof and wall to the foundation. More modeling details related to the element selection and connection refer to He *et al.* (2018). Totally, the model is created by 12,901 beam elements, 39,505 shell elements, and 50,664 nonlinear spring elements.

2.2 Wind loading

The Boundary Layer Wind Tunnel at LSU is an open return wind tunnel with a test section of 2.44 m (8 ft) in length, 1.32 m (4.3 ft) in width, and 0.99 m (3.2ft) in height and it is powered by a 2.4 m (7.9 ft) diameter fan that is capable of producing a free stream velocity of up to 12 m/s (Gregg 2006). An open terrain atmospheric boundary layer with a roughness length z_0 of 0.0142 m is simulated by setting roughness elements such as carpet on the floor,

spires at the entrance, and saw tooth trip in the downstream from spires. The external pressure datasets for the LSU aerodynamic database are collected under three angles, namely 0° , 45° , and 90° which roughly covers the entire angle range due to the symmetric building geometry. For the internal pressure measurements, the volume scaling is considered by adding an internal volume chamber to the building model. More details about the scaling as well as the internal volume chamber can be found in Pan *et al.* (2013). These internal pressure datasets are tested under eight wind angles over a 360° range at 45° increments with different opening cases, some of which have been published by Pan *et al.* (2013).

For the comparison of wind effects with the ASCE 7 provisions, four loading cases based on the DAD methodology were carried out in the current study that employs the pressure datasets from the LSU aerodynamic database, as illustrated in Table 1. All these cases apply the external dynamic pressures from LSU database with a duration of 2s of stable records to reduce the computation effort. The internal pressure datasets from LSU are used for the first case subjected to a wind angle of 90° to evaluate the internal pressure effects as opposed to the previous ASCE 7 evaluation research with the DAD method that focused only on comparing the external pressure effects and used the standard defined internal pressures such as Coffman *et al.* (2010). The ASCE 7 defined internal pressure coefficients are used for the rest cases covering all three angle cases of external pressure in the LSU database for consistency. Finally, the DAD responses used for the comparisons with the ASCE 7 are the peak values, positive and negative, of all the three DAD cases using the ASCE 7 internal pressure (DAD2 to DAD4). The comparisons among these four DAD cases (DAD1 to DAD4) are also discussed and detailed later to investigate the wind directional effects and code-based internal pressure coefficients effects. It is noted that in this study, we focus on the difference of DAD and ASCE 7 based on the external pressure. Therefore, we use the peak value of DAD2-DAD4, (LSU wind tunnel external pressure time-

histories but ASCE-7 internal pressure) to compare with the ASCE 7 predicted value. Then, we compare DAD1 (90°) and DAD2 to DAD4 loading cases to demonstrate that if LSU wind internal pressure is used, the difference between DAD and ASCE 7 can be even more significant. The DAD1 (90°) is chosen to compare with its counterpart loading case DAD4 and the other cases because this 90° angle loading case produces the largest internal pressure (Pan *et al.* 2013).

In order to compare with the wind effect of the ASCE 7-10 provisions, the pressure coefficient measures from the LSU wind tunnel referenced to the mean roof height pressure are re-normalized to the storm condition specified in the ASCE 7-10 of a 3-s gust wind speed at 33 ft (10 m) in an open terrain (roughness length $z_0=0.03$ m, Table C26.7-2, ASCE 7-10).

$$\begin{aligned} C_{p,3s,10m,z_0=0.03m} &= C_{p,ref} \times \left(\frac{q_{ref}}{q_{3s,10m,z_0=0.03m}} \right) \\ &= C_{p,ref} \times \left(\frac{V_{ref}}{V_{3s,10m,z_0=0.03m}} \right)^2 \end{aligned} \quad (1)$$

where

$$C_{p,ref} = \frac{p}{q_{ref}} = \frac{p_i - p_0}{q_{ref}} \quad (2)$$

$$\begin{aligned} &\left(\frac{V_{ref}}{V_{3s,10m,z_0=0.03m}} \right)^2 \\ &= \left(\frac{V_{ref}}{V_{1h,10m,z_0=0.0142m}} \right)^2 \\ &\times \left(\frac{V_{1h,10m,z_0=0.0142m}}{V_{3s,10m,z_0=0.0142m}} \right)^2 \\ &\times \left(\frac{V_{3s,10m,z_0=0.0142m}}{V_{3s,10m,z_0=0.03m}} \right)^2 \end{aligned} \quad (3)$$

In Eq. (1), $C_{p,3s,10m,z_0=0.03m}$ is the normalized wind pressure coefficient; $C_{p,ref}$ is the pressure coefficient at the reference height, testing terrain, and testing wind speed; q_{ref} is the dynamic pressure at the upper level reference height in the wind tunnel measured by the pitot tube; and $q_{3s,10m,z_0=0.03m}$ is the dynamic pressure at the storm condition (i.e., 3-s gust wind, 10 m reference height and terrain roughness length z_0 of 0.03 m) that is consistent with that defined in the ASCE 7-10. In Eq. (2), p represents the net tap pressure and is expressed by the difference between the model surface pressure measured by the pressure taps p_i and the reference level static pressure p_0 simultaneously derived from the Pitot tube. The first term in Eq. (3) represents the adjustment for height and is obtained from the velocity profile measured by Pan *et al.* (2013); the second term adjusts for the average time taken from the ‘‘Durst Curve’’ in Fig. C26.5-1, ASCE 7-10; and the last ratio adjusting for terrain is obtained from the Engineering Science Data Unit (ESDU 1990) model.

Table 1 DAD Loading Cases

Case No.	Wind Angle	External Pressure	Internal Pressure
DAD1	90°	LSU	LSU
DAD2	0°	LSU	ASCE 7-10
DAD3	45°	LSU	ASCE 7-10
DAD4	90°	LSU	ASCE 7-10

The pressure coefficients measured on the pressure taps are then discretized to be applied to their tributary area on the refined finite-element (FE) model, and the applied wind pressures is calculated by Eq. (4) for a 44.7 m/s (115 mph) basic wind speed used in the ASCE 7. Pressures in the form of time histories from the LSU database are used here as a DAD method to evaluate the ASCE 7 provision.

$$P = \frac{1}{2} \rho V_{3s,10m,z_0=0.03m}^2 [C_{pe,3s,10m,z_0=0.03m} - C_{pi,3s,10m,z_0=0.03m}] \quad (4)$$

3. Comparison with ASCE 7-10 Provisions

The critical members of a low-rise building subjected to wind loads can be classified into either the MWFRS or the C&C based on the definitions given in the standard. Therefore, the critical demands corresponding to the ASCE 7-10 are calculated following the analytical methods for the two systems. It states that components can be part of the MWFRS when they act as shear walls or roof diaphragms that transfer wind loads to the ground. For the roof truss system, the long-span trusses should be designed based on the MWFRS method, and the individual member of trusses should be designed by the C&C method (Mehta and Marshall 1998). Morrison (2010) suggested the toe-nail RTWCs in building models should be treated in both ways as it is unclear which category they should be classified to. Mensah *et al.* (2011) and Roueche *et al.* (2015) also applied both methods to the design of the RTWCs and wall-to-foundation connections (WTFs) in an entire building, and compared the wind effects between the ASCE 7-10 and DAD directly. It is noteworthy that the loads specified in the C&C method are not intended to be used when considering the effects of loads from multiple surfaces, not to mention to be applied to an entire building. As such, if do so, one can expect larger structural response on the component or cladding by following the C&C procedure. However, in the present analysis, both types of procedures, MWFRS (ASCE7-10 sect.27.4.1 and ASCE7-10 sect. 28.4.1) and C&C (ASCE7-10 sect.30.4.1) are applied. The results of them would provide a range of the ASCE7-10 predictions and a more direct comparison to quantify the differences.

According to the ASCE 7, the current building model is regarded as enclosed by its opening arrangement, and the internal pressure coefficient, (GC_{pi}) , is ± 0.18 for this enclosure classification. The basic parameters such as wind

directionality factor (K_d) and the topographic factor (K_{zt}) are 0.85 and 1.0, respectively. All the possible loading scenarios of the three procedures in ASCE 7, namely the Directional Procedure, the Envelope Procedure, and the C&C method are listed in Table 2 considering the symmetry of the building.

4. Discussion

4.1 Critical demands comparison

Table 3 lists the positive and negative peak responses obtained through various ASCE 7 procedures and wind tunnel loadings for the low-rise wood frame building stated under the 44.7 m/s (115 mph) ASCE 7 basic wind speed. The responses include the peak sheathing displacement, a representative indicator of the failure of wood houses on the roof, and the peak uplift forces at all the critical connections including the STTCs, RTWCs, and WTFCs. The positive

and negative peak values of the sheathing displacement represent the displacement perpendicular to the roof surface out of and into the building, respectively. The positive uplift force at all the connections represents the vertical forces to stretch the connections that would cause failure. The negative value means the forces to push the sheathing to the truss, the roof assemblies to the wall, and the entire building to the foundation for the STTCs, RTWCs, and WTFCs, respectively. Thus, the negative value is not our primary concern. These selected structural responses are taken as the code performance indicators to explore how applicable of the ASCE 7 procedures to the light-frame wood house, a different structural system from industrial buildings. The peak values of these code indicators calculated with the DAD methodology under loading cases DAD2-DAD4 are compared to the predictions based on all the procedures provided in the ASCE 7.

As it is shown in the table, the design based on the ASCE 7 wind loads are not always conservative based on the positive values of the results under the wind speeds discussed. The maximum uplift forces on the RTWCs based on the DAD method are lower than the Envelope Procedure and C&C method induced values, with the ratio being 0.9 and 0.8, respectively. For the uplift force on the WTFCs, the DAD prediction is lower than the maximum result of the C&C method with their ratio being 0.8. However, for all the other code performance indicators, the DAD predicted maximum reactions are higher including the uplift force on the STTCs and the displacement on the sheathing, which are more influenced by the local pressures. Of the three critical connections, the ratio in the STTCs between the DAD and ASCE 7 maximum predictions of all cases (i.e., D, E, and C&C) varies from 1.1 to 2.8 that are larger than the differences in the RTWCs and WTFCs, with the ratios both being 0.8-1.6. Since the DAD prediction employs the actual measured wind loading, this large discrepancy on the responses of the STTCs between the ASCE 7 design and the DAD predictions indicates the insufficiency of the ASCE 7 design, especially on the roof envelope. Such design procedure makes the roof sheathing nail the most vulnerable component for the winds encountered. This vulnerability is consistent with most common damage being the roof sheathing blown off reported by the past reconnaissance such as the Mitigation Assessment Team deployed by the Federal Emergency Management Agency's (FEMA's) Mitigation Division (e.g., FEMA 2005). In looking at Table 3, for a wind direction that results in the peak uplift force at the STTCs, all peak responses were observed in the range of 45°~90°, i.e., 90° for the directional procedure, Load Case A (45°~90°) for the envelope procedure, and 45° for DAD method. This emphasizes the importance of the wind directional effects on the roof where the pressure distribution is greatly determined by the separation of flow at the windward edges and the secondary flow separation at the ridge in accordance with the wind direction.

For the negative peak values, ASCE 7 predictions are larger than the DAD results and are conservative for most critical demands only except the STTC uplift force. However, in every case, these negative peak values are of considerably less magnitude than their positive

Table 2 ASCE 7 Load Case Applied

Combination	Wind Direction ^a	Internal Pressure ^b	Condition ^c
Directional			
D1	N	-	1
D2	N	-	2
D3	N	+	1
D4	N	+	2
D5	P	-	N/A
D6	P	+	N/A
Envelope			
E1	A	-	N/A
E2	A	+	
E3	B	-	
E4	B	+	
C&C			
C1	N	-	N/A
C2	N	+	
C3	O	-	
C4	O	+	
C5	P	-	
C6	P	+	

^a N = normal to roof ridge and P = parallel to roof ridge for Directional Procedure (Fig. 27.4-1 in ASCE 7-10); A and B for Envelope Procedure refer to Load Case A (45°-90°) and Load Case B (0°-45°) (Fig. 28.4-1 in ASCE 7-10); P, O, and N denotes parallel, oblique, and normal to roof ridge for C&C procedure.

^b Internal pressure corresponds to the enclosed enclosure classification with pressure coefficient (GC_{pi}) = ± 0.18 , where the plus and minus signs signify pressures acting toward and away from the surfaces, respectively.

^c Conditions 1 and 2 refer to the two values of external pressure coefficient for the windward roof in ASCE 7-10 (Fig. 27.4-1).

Table 3 Peak Response in Critical Members discussed under Cat. 2 SSHWS: 115 mph ASCE 7 Wind Speed

Case	Peak Type	Sheathing Displacement (m)			STTC Uplift (N)			RTWC Uplift (N)			WTFC Uplift (N)		
		DAD	ASCE	Ratio	DAD	ASCE	Ratio	DAD	ASCE	Ratio	DAD	ASCE	Ratio
D1	+	4.0E-02	8.6E-03	4.7	1041.3	218.0	4.8	4555.6	1315.3	3.5	8693.8	3484.0	2.5
	-	-7.9E-03	-2.4E-03	3.4	-608.1	-126.3	4.8	N/A	N/A	N/A	-4416.6	-3014.0	1.5
D2	+		8.9E-03	4.5		366.1	2.8		1017.4	4.5		5047.3	1.7
	-		-8.6E-03	0.9		-220.9	2.8		N/A	N/A		-5368.0	0.8
D3	+		1.6E-02	2.5		435.4	2.4		2827.6	1.6		5574.1	1.6
	-		-2.4E-03	3.3		-215.0	2.8		N/A	N/A		-2629.1	1.7
D4	+		1.6E-02	2.5		428.7	2.4		2488.3	1.8		5503.6	1.6
	-		-4.0E-03	2.0		-209.2	2.9		N/A	N/A		-4710.3	0.9
D5	+		2.3E-03	17.7		163.6	6.4		536.8	8.5		2654.5	3.3
	-		-1.3E-03	6.2		-145.1	4.2		N/A	N/A		-1794.5	2.5
D6	+		7.3E-03	5.5		180.9	5.8		1539.0	3.0		3318.2	2.6
	-		-2.0E-03	3.9		-148.5	4.1		N/A	N/A		-1997.1	2.2
Mean Value	+			6.2			4.1			3.8			2.2
	-			3.3			3.6			N/A			1.6
E1	+		1.1E-02	3.7		288.9	3.6		2439.3	1.9		3701.4	2.3
	-		-3.5E-04	22.6		-140.8	4.3		N/A	N/A		N/A	N/A
E2	+		1.8E-02	2.2		506.4	2.1		4184.3	1.1		6522.8	1.3
	-		-3.5E-04	22.6		-249.1	2.4		N/A	N/A		N/A	N/A
E3	+		1.7E-02	2.3		256.5	4.1		3555.7	1.3		5818.4	1.5
	-		-2.5E-03	3.2		-315.6	1.9		N/A	N/A		-2530.1	1.7
E4	+		2.4E-02	1.6		473.9	2.2		5262.1	0.9		8304.5	1.0
	-		-2.5E-03	3.2		-369.1	1.6		N/A	N/A		-2367.1	1.9
Mean Value	+			2.5			3.0			1.3			1.6
	-			12.9			2.6			N/A			1.8
C1	+		2.8E-02	1.4		709.2	1.5		4190.2	1.1		8385.7	1.0
	-		N/A	N/A		-424.5	1.4		N/A	N/A		N/A	N/A
C2	+		3.3E-02	1.2		927.2	1.1		5431.7	0.8		11182.9	0.8
	-		-6.2E-05	127.3		-489.5	1.2		N/A	N/A		N/A	N/A
C3	+		2.9E-02	1.4		635.6	1.6		3798.3	1.2		8660.7	1.0
	-		-1.0E-02	0.8		-420.2	1.4		N/A	N/A		-5067.9	0.9
C4	+		3.4E-02	1.2		853.7	1.2		4708.5	1.0		11011.0	0.8
	-		-3.8E-03	2.1		-476.3	1.3		N/A	N/A		-4488.4	1.0
C5	+		2.9E-02	1.4		462.4	2.3		3198.7	1.4		8157.8	1.1
	-		-1.1E-02	0.7		-474.9	1.3		N/A	N/A		-6821.9	0.6
C6	+		3.4E-02	1.2		670.5	1.6		4523.5	1.0		9020.9	1.0
	-		-6.6E-03	1.2		-534.2	1.1		N/A	N/A		-6528.7	0.7
Mean Value	+			1.3			1.5			1.1			0.9
	-			22.0			1.3			N/A			0.8

Note:

The highlighted values are the positive and negative peak values for each ASCE 7 procedure, i.e., D, E, and C.

Ratio=DAD/ASCE. The Ratios less than 1 are highlighted by squares and represent the ASCE 7 design is conservative.

counterparts. Therefore, the efficient capacities and schedules of sheathing nails and frame connections that are sufficient for the positive peak responses should also be sufficient for these smaller negative peak values.

The peak values (positive and negative) of all the cases for each ASCE 7 procedure are compared with the corresponding DAD results in Fig. 3. Generally speaking, the absolute maximum responses based on Envelope Procedure are larger than the Directional Procedure results and closer to the results based on the DAD methodology. The Envelope Procedure developed by enveloping the critical demands such as the moments is also better at predicting the critical structural actions such as the uplift force at connections with closer results to the DAD predictions than the Directional Procedure for the light frame wood buildings. For the critical structural actions

mainly subjected to local pressures such as the peak uplift force on the STTCs, the two MWFRS procedures (directional and envelope) predict similar values. The results based on the C&C method is larger than the MWFRS methods at all the critical demands as expected. However, even though conceptually using the C&C method should have overestimated the system effect of the structure, the responses such as the STTC uplift force induced by this method is still smaller than the DAD results indicating the nonconservatism aspect of the design provision.

4.2 Critical location/ Critical member comparison

Fig. 4 demonstrates the locations of the critical members that are determined by the load distribution for all the peak

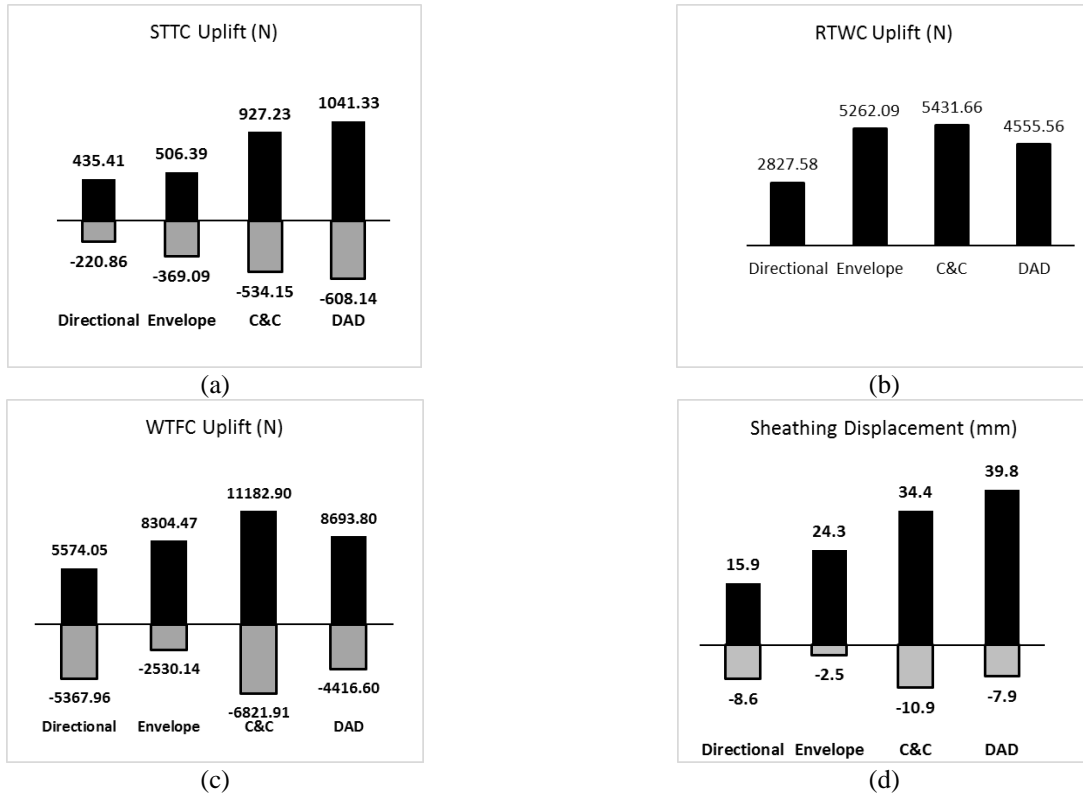


Fig. 3 Critical demands for residential structures based on ASCE 7 and DAD procedures at sheathing panels, STTCs, RTWCs, and WTFCs (115mph)

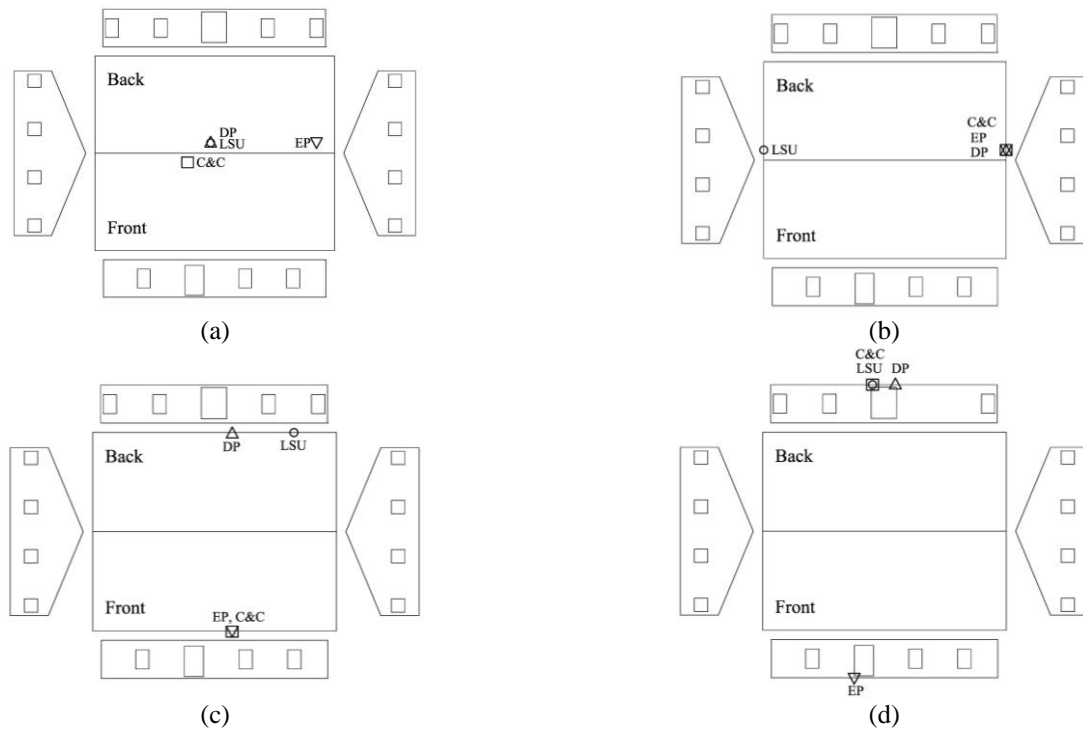


Fig. 4 Locations of the critical demands for residential structures (115mph): (a) sheathing panels; (b) STTCs; (c) RTWCs; and (d) WTFCs. (DP: Directional Procedure; EP: Envelope Procedure; C&C: C&C method; LSU: DAD method based on the LSU database)

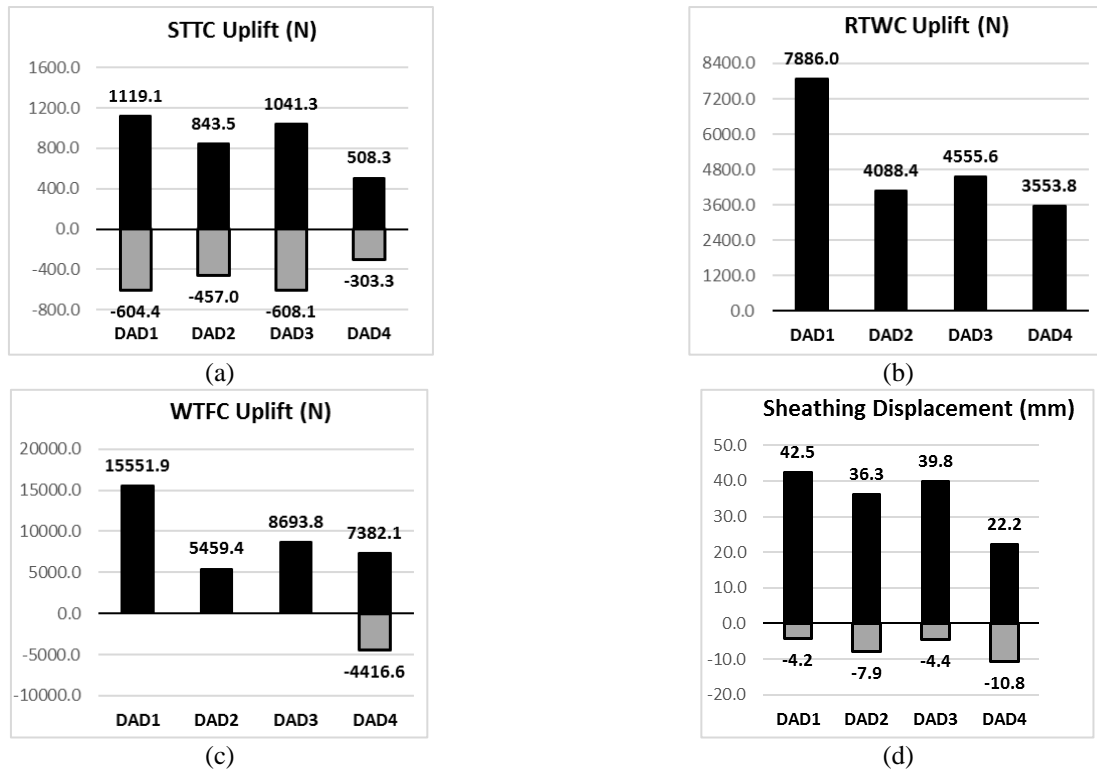


Fig. 5 Critical demands predicted by DAD loading cases (115 mph)

actions discussed here. For the sheathing displacement as shown in Fig. 4(a), the DP makes a same prediction on the critical member as the DAD (LSU) prediction with the location being near the middle of the ridge on the leeward roof. The C&C method prediction is around the similar area, but on the opposite side of the roof; the EP predicts the largest sheathing displacement happening on the same side as the DAD prediction while close to the head of the ridge. For the critical location of sheathing panel where the largest sheathing displacement is, both the predictions made by the ASCE 7 procedures and DAD method are around the roof ridge.

Besides the critical envelope components, the critical connections are discussed. Fig. 4(b) shows that for the sheathing nail experiencing the largest uplift force, all the three procedures of the ASCE 7 point to the same critical member that is on the leading edge near the ridge. In comparison, the LSU critical point is on the other end edge that is symmetric about the center line of the building in the gable wall direction. Both the critical STTCs predicted by ASCE 7 and DAD method are located on the edge of roof by the gable wall while on the opposite side. In Fig. 4(c), the critical RTWCs under the ASCE7 procedures are on the same truss but different ends: the members based on the EP and C&C method are on the wind ward end and the DP prediction is on the other end. The DAD prediction of the critical RTWC is on the leeward side but closer to the gable end, which makes the DP a closer prediction on the same side of the roof. Being the last structural member along the load path, the critical WTFC predicted by all the methods

are on the wall studs by the large openings as shown in Fig. 4(d), i.e., front and back door, which is partly accounted for by the fact that there are WTFCs right under every stud in this current model. Overall, the Directional Procedure is found to yield closer predictions on the critical members to the DAD predictions, indicating the load distribution defined in the Directional Procedure is closer to the actual one.

4.3 Wind directional effects and code-based internal pressure coefficients

The structural responses under all the four DAD loading cases detailed in Table 1 are shown in Fig. 5. The DAD1 predictions using wind tunnel measured internal pressures under 90° winds are plotted in the same figure as the rest DAD predictions that employ the ASCE 7 internal pressure values to illustrate the discrepancy induced by using different internal pressure coefficients. This item also serves as a reference to deduce the peak realistic structural responses under other wind directions. The peak responses predicted by DAD1 loading cases have increased, compared with their counterparts based on DAD4, by 120%, 122%, 11%, and 91% for the STTC uplift force, RTWC uplift force, WTFC uplift force, and sheathing displacement, respectively. These larger discrepancies are induced by the larger internal pressures measured in wind tunnel. This indicates that the underprediction of the ASCE 7 illustrated earlier can be even more significant based on realist internal wind loads.

Among the loading cases using the ASCE 7 internal pressures, i.e., DAD2-DAD4 as shown in Figs. 5(a)-5(d), the peak values of all the demands for residential houses considered here are obtained under oblique incident winds, i.e., 45°. As such, in terms of the critical wind direction, the ASCE 7 provision is not applicable to the residential house design.

5. Conclusions

This study evaluated the adequacy of wind design by using the ASCE 7-10 wind provisions on residential buildings. A review of the methodologies behind the ASCE 7-10 procedures showed a great gap between the industrial building type which the code is developed upon and the residential constructions with different configurations, namely material property and inter-connections. Based on the discussions of the present study, the following can be concluded and recommended.

- The adequacy of the ASCE 7 methods, including the Directional Procedure and Envelope Procedure for MWFRS and the C&C method, to the design of low-rise wood buildings in terms of matching critical structural actions calculated from the actual wind tunnel loading is not a clear cut. The Directional Procedure is found to be consistently unconservative; the Envelope Procedure may over predict or predict close critical actions at the RTWCs and WTFCs while not sufficient for the responses governed by local pressures such as the uplift force on the STTCs. The C&C method that has incorporated the system effects is conservative for most actions as expected except the STTC uplift indicating the even larger underestimations of the ASCE 7 on these demands. As stated above, the design of ASCE 7 is unconservative especially on the vulnerable STTCs. Therefore, for the structural actions determined more by local wind pressures, the design that follows the ASCE 7 provisions has a great chance of being unconservative.
- Between the two procedures for the MWFRS, the Directional Procedure represents envelopes of the real wind loads acting on the building as opposed to the Envelope Procedure that uses the fictitious load fitted from the values of postulated critical reactions. Therefore, the wind effect followed by the Directional Procedure will not be influenced by the load paths and sharing of a specific configuration, and less difference is expected from that of DAD. However, the Envelope Procedure is found to result in higher response and be generally better at predicting the critical demands for wood houses compared with the DAD approach than the Directional Procedure in the sense of magnitude. Regarding the location of the critical member, the Directional Procedure does a better job.
- For the loading scenarios considered, the critical wind angle that may trigger the first failure of wood framed buildings on the vulnerable members including the sheathing panels, the STTCs, the RTWCs and the WTFCs is found to be oblique, i.e., 45°.

- To allow the ASCE 7 provisions to be confidently used on wood residential houses, research should be undertaken for a more comprehensive set of comparisons in the future for buildings with various geometries and wider potential critical actions. The methodology to envelop the critical reactions is superior in targeting directly at the structural response, but it is limited in exhausting all the constantly evolving structural configurations. A new methodology is expected to revise the ASCE 7 wind loads code that can inherit the merits of both the current procedures to eliminate the underestimation of wind effects and reflect the critical member under wind loads.

Acknowledgements

This work is partially supported by the NSF project No. CMMI-1233991 and Louisiana State University under the Economic Development Assistantship for the first author. These supports are greatly appreciated. The contents of the paper reflect only the views of the authors.

References

- ASCE (2010), "Minimum Design Loads for Buildings and Other Structures", ASCE/SEI 7-10, Reston, VA.
- Coffman, B.F., Main, J.A., Duthinh, D. and Simiu, E. (2010), "Wind effects on low-rise buildings: database-assisted design versus ASCE 7-05 Standard estimates", *J. Struct. Eng.*, **136**(6), 744-748.
- Cook, R.A. and Soltani, M. (1994), "Hurricanes of 1992", American Society of Civil Engineers, New York, NY.
- Davenport, A.G., Surry, D. and Stathopoulos, T. (1978), "Wind loads on low-rise buildings", Final report on phase III, BLWT-SS4; Univ. of Western Ontario, London, ON, Canada.
- Douglas, B.K. and Weeks, B.R. (2003), "Considerations in wind design of wood structures", AF&PA, Washington, DC.
- Engineering Science Data Unit (ESDU) (1990), "Strong Winds in the Atmospheric Boundary Layer. Part 1. Mean-Hourly Wind Speeds", Data Item 82026.
- Federal Emergency Management Agency (FEMA) (1993), "Hurricane Andrew in Florida, Report #22", Washington, D.C.
- Federal Emergency Management Agency (FEMA) (2005), "Hurricane Charley in Florida, Report #488", Washington, D.C.
- Fischer, C. and Kasal, B. (2009), "Analysis of light-frame, low-rise buildings under simulated lateral wind loads", *Wind Struct.*, **12**(2), 89-101.
- Gavanski, E., Kordi, B., Kopp, G.A. and Vickery, P.J. (2012), "Wind loads on roof sheathing of houses", *J Wind Eng. Ind. Aerod.*, **114**, 106-121.
- Gregg, J.P. (2006), "Development and application of methods for evaluation of hurricane shelters", M.S. Thesis, Louisiana State University, Baton Rouge, LA.
- He, J., Pan, F. and Cai, C.S. (2017), "A review of wood-frame low-rise building performance study under hurricane winds", *Eng. Struct.*, **141**, 512-529.
- He, J., Pan, F., Cai, C.S., Chowdhury, A. and Habte, F. (2018), "Finite-element modeling framework for predicting realistic responses of light-frame low-rise Buildings under wind loads", *Eng. Struct.*, **164**, 53-69.
- Isyumov, N. and Case, P. (1995), "Evaluation of structural wind Loads for low-rise buildings contained in ASCE Standard 7-1995 (Feb. 1995 draft)", BLWT-SS17-1995, Univ. of Western

- Ontario, ON, Canada.
- Jacklin, R.B., El Damatty, A. and Dessouki, A. (2014), "Finite-element modeling of a light-framed wood roof structure", *Wind Struct.*, **19**(6), 603-621.
- Kopp, G.A., Surry, D. and Mans, C. (2005), "Wind effects of parapets on low buildings: Part 1. Basic aerodynamics and local loads", *J Wind Eng. Ind. Aerod.*, **93** (11), 817-841.
- Kwon, D.K., Kareem, A., Kumar, D. and Tamura, Y. (2016), "A prototype online database-enabled design framework for wind analysis/design of low-rise buildings", *Front. Struct. Civil Eng.*, **10**(1), 121-130.
- Martin, K.G., Gupta, R., Prevatt, D.O., Datin, P.L. and van de Lindt, J.W. (2011), "Modeling system effects and structural load paths in a wood-framed structure", *J. Archit. Eng.*, **17**(4), 134-143.
- Mehta, K.C. and Marshall, R.D. (1998), "Guide to the use of the wind load provisions of ASCE 7-95", American Society of Civil Engineers Press, Reston, Va.
- Mensah, A.F., Datin, P.L., Prevatt, D.O., Gupta, R. and van de Lindt, J.W. (2011), "Database-assisted design methodology to predict wind-induced structural behavior of a light-framed wood building", *Eng. Struct.*, **33**, 674-684.
- Morrison, M.J. (2010), "Response of a two-story residential house under realistic fluctuating wind loads", PhD Thesis, Department of Engineering, The University of Western Ontario, London, Ontario, Canada
- Pan, F, Cai, C.S. and Zhang, W. (2013), "Wind-induced internal pressures of buildings with multiple openings", *J. Eng. Mech.*, **139**(3), 376-385.
- Pielke, R.A. and Landsea, C.W. (1998), "Normalized hurricane damages in the United States, 1925- 1995", *Weather Forecast.*, 621-631.
- Reinhold, T.A. (2005), "Assessing the performance of modern building codes & standards in reducing hurricane damage", Presentation for Meeting of Task Force on Long-Term Solutions Florida's Hurricane Insurance Market.
- Roueche, D.B., Prevatt, D.O., Haan, F.L. and Datin, P.L. (2015), "An estimate of tornado loads on a wood-frame building using database-assisted design methodology", *J. Wind Eng. Ind. Aerod.*, **138**, 27-35.
- Shanmugam, B., Nielson, B.G. and Prevatt, D.O. (2009), "Statistical and analytical models for roof components in existing light-framed wood structures", *Eng. Struct.*, **31**, 2607-2616.
- Sparks, P.R. (1991), "Hurricane Hugo in perspective", NIST Special Publication 820, National Institute of Standards & Technology, 29-37.
- St. Pierre, L.M., Kopp, G.A., Surry, D. and Ho, T.C.E. (2005), "The UWO contribution to the NIST aerodynamic database for wind loads on low buildings. 2: Comparison of data with wind load provisions", *J. Wind Eng. Ind. Aerod.*, **93**(1), 31-59.
- Tieleman, H., Elsayed, M. and Hajj, M. (2006), "Peak wind load comparison: Theoretical estimates and ASCE 7", *J. Struct. Eng.*, **132**(7), 1150-1157.
- Trautner, C. and Ojdrovic, R. (2013), "Comparison of directional and envelope wind load provisions of ASCE 7", *J. Struct. Eng.*, **140**(4).
- van de Lindt, J. and Dao, T. (2009), "Performance-based wind engineering for wood-frame buildings", *J. Struct. Eng.*, **135**(2), 169-177.